IEEE Access
Multidisciplinary | Rapid Review | Open Access Journal

Received November 6, 2020, accepted November 21, 2020, date of publication November 27, 2020,
date of current version December 9, 2020.

Digital Object Identifier 10.1109/ACCESS.2020.3041158

Principal Motion Ellipsoids: Gait Variability Index Invariant With Gait Speed

TOMOYUKI IWASAKI, SHOGO OKAMOTO, (Member, IEEE), YASUHIRO AKIYAMA, (Member, IEEE), AND YOJI YAMADA, (Member, IEEE)
Department of Mechanical Systems Engineering, Nagoya University, Nagoya 464-8603, Japan

Corresponding author: Shogo Okamoto (shogo.okamoto@mae.nagoya-u.ac.jp)

This work was supported in part by the Japan Agency for Medical Research and Development (AMED) under Grant 19he2002003h0302, and in part by the JSPS KAKENHI under Grant 19K21584.

ABSTRACT The walking motion of an individual involves considerable variability. We develop a gait variability index that determines how and to what degree repeated human gait motions vary, based on generalized principal motion analysis (GPMA). Principal motion analysis (PMA) is an extension of principal component analysis and decomposes multivariate time-series data, such as human joint angles during walking, into a linear combination of several principal motion bases. The developed gait variability index is defined by the size of an ellipsoid referred to as a PM ellipsoid and approximates the distribution of repeated gait motions on the motion base space. We expand the method to compute PM ellipsoids using GPMA, which enables us to mask the effects of a certain factor affecting gait motion observed under multiple factors. We compute the principal motion bases invariant with the gait speed from the gait motions of nine participants at two speed levels, 3.5 and 4.0 km/h. The sizes of the PM ellipsoids computed using GPMA do not depend on the gait speed and exhibit good agreement with the MeanSD, i.e., a typical gait variability index with correlation coefficients greater than 0.87.

INDEX TERMS Gait speed, modal analysis, walking motion, principal motion analysis.

I. INTRODUCTION

There is large variability in the walking motion of an individual. For example, the gait of a human varies depending on the gait speed [1], [2] and step length [3], [4] during walking. Some studies have discussed the gait variability in individuals during curving motion [5], [6]. The MeanSD [7] and maximum Lyapunov exponent [8] are the most popular indices for evaluating gait variability. MeanSD is the mean value of the standard deviation of parameters, such as joint angles. The maximum Lyapunov exponent, which is also used as a gait stability index, quantifies the average logarithmic rate of the divergence of a system after perturbation. If the values of these indices are large, the gait variability in an individual is considerable. In addition, multiscale entropy [9] and recurrence quantification analysis [10] have been reported as highly reproducible indices [11]. Thus, gait variability has been extensively studied. Indices to represent gait variability are invaluable in enhancing commercial applications, such as walking aids, and in the clinical scenario [12], [13] where gait variability is an important characteristic of neurological disorders [14]. However, as these indices are represented by single scalar quantities, they are unsuitable for discussing the variation in walking motion, although they are suitable for discussing the level of gait variability.

Human motion has been analyzed through principal motion analysis (PMA) [15], [16], also called principal component analysis for time-series [17]–[24] or spectral analysis [25]. This method decomposes human motion into bases called principal motions or synergies without losing information on the interlocked multiple degrees of freedom of redundant systems. It reduces the entire body motion to a few-dimensional parameter space, and has mainly been applied for understanding motion synergies [17]–[25] and generating human and robot motions [15], [16], [26]–[28]. PMA has also been adapted to classify individual gait [29], [30] and sit-to-stand motion [31].

We had previously proposed the principal motion ellipsoid (PM ellipsoid) as an index for the gait variability [32]. This ellipsoid is an error ellipsoid calculated from the

The associate editor coordinating the review of this manuscript and approving it for publication was Zhong Wu.

distribution of the principal motion scores. Conventional indices aim to represent the variability as a scalar quantity. In contrast, the PM ellipsoid can analyze it as a multivariate time-series. The variation in the walking motion of an individual can be determined by interpreting the obtained principal motions [32]. Furthermore, the size of the PM ellipsoid represents the level of variability of individual motion and exhibits high correlation with the MeanSD.

Gait speed has considerable effect on the walking motion; hence, it may not be possible to investigate individual walking motion, if the gait speed is not suitably controlled. Some of the gait characteristic quantities vary significantly under different gait speeds [4], [33]–[38]. PMA explores base functions that maximize the variability among all the samples. Hence, when the gait speed is not controlled among all the samples, the base functions are sensitive to not only the individual characteristic walking motion but also the gait speed. Therefore, PMA cannot be applied for identifying the principal motions in experiments involving uncontrolled gait speed.

Generalized principal motion analysis (GPMA) is a method for extracting the principal motions related to specific experimental factors [31]. Gait motion comprises multiple factors such as individual differences, gait speed, and repetition errors. GPMA can mask the effects of some of these motion factors, and extract the corresponding invariant principal motions. For example, the masking of repetitive errors in sit-to-stand motion has been demonstrated, and individuals within a group have been classified [31].

In this study, we develop a new PM ellipsoid based on GPMA, combining [31] and [32]. As mentioned above, the PM ellipsoid is advantageous because it can analyze the variation in the walking motion and the phase at which it occurs within the gait cycle. Furthermore, a GPMA-based PM ellipsoid can mask specific factors among the motion samples, such as the gait speed, whereas the afore-mentioned indices [7]–[10], [32] do not aim to mask the effects of certain factors. For example, the maximum Lyapunov components [4], [36], variabilities in the step length, interval [34], and stride time [37], and MeanSD [37], [38], all of which are used as gait variability indices, are sensitive to the gait speed, whereas the step-length variability may not be affected by the gait speed [37], [39]. The existing popular gait variability indices are sensitive to the gait speed. In contrast, PM ellipsoids based on GPMA can be employed as a gait variability index invariant with the gait speed. However, when GPMA is applied, the principal motions may not be easy to interpret because of its strong masking ability. Therefore, in this study, we extend GPMA to introduce a method for adjusting its masking ability.

II. MOTION ANALYSIS METHODS

A. PRINCIPAL MOTION ANALYSIS (PMA)

Principal motion analysis (PMA) is an extension of principal component analysis, which deals with multivariate time-series data [15]–[29]. It extracts covariation sets in the temporal dimension, among multiple variables. Each set is called principal motion and the sets are linearly independent of each other. PMA is a linear analysis method, and it is relatively easy to interpret the meaning of the obtained principal motions.

Suppose that a human motion at a certain instant is represented by p variables. For variable i ($i = 1, \ldots, p$) at the k-th trial ($k = 1, \ldots, k'$), the time-series data vector $\boldsymbol{\theta}_{i,k}$ comprising discretized u moments is

$$\boldsymbol{\theta}_{i,k} = (\theta_{i,k,1}, \theta_{i,k,2}, \ldots, \theta_{i,k,u}). \tag{1}$$

Using this, we create an extended column vector $\boldsymbol{x}_k$ ($\in \mathbb{R}^{pu\times 1}$) including p variables:

$$\boldsymbol{x}_k = (\boldsymbol{\theta}_{1,k}, \ldots, \boldsymbol{\theta}_{i,k}, \ldots, \boldsymbol{\theta}_{p,k})^{\mathrm{T}}. \tag{2}$$

Note that $\boldsymbol{x}_{c,k}^{(s)}$ represents the time-series column vector of experimental participant s ($s = 1, \ldots, s'$) at the k-th trial under condition c ($c = 1, \ldots, c'$). If we obtain k' sets of walking motion from each of the s' participants under c' conditions as the motion samples, the time-series data of all the motions are represented by matrix $\boldsymbol{X}$ ($\in \mathbb{R}^{s'c'k'\times pu}$) as follows:

$$\boldsymbol{X} = (\boldsymbol{x}_{1,1}^{(1)}, \ldots, \boldsymbol{x}_{c,k}^{(s)}, \ldots, \boldsymbol{x}_{c',k'}^{(s')})^{\mathrm{T}}. \tag{3}$$

From the eigenvector expansion of covariance matrix $\boldsymbol{X}$, we obtain

$$\boldsymbol{X} \sim \boldsymbol{Y}\boldsymbol{V}^{\mathrm{T}}, \tag{4}$$

where $\boldsymbol{Y} = (\boldsymbol{y}_{1,1}^{(1)}, \ldots, \boldsymbol{y}_{c'k'}^{(s')})^{\mathrm{T}}$ ($\in \mathbb{R}^{s'c'k'\times r}$) is a score matrix that represents the quantity of information of each principal motion included by each observed motion and $\boldsymbol{V} = (\boldsymbol{v}_1, \ldots, \boldsymbol{v}_q, \ldots, \boldsymbol{v}_r)$ ($\in \mathbb{R}^{pu\times r}$) is a principal motion matrix composed of r eigenvectors corresponding to the r largest eigenvalues; $\boldsymbol{v}_q$ ($\in \mathbb{R}^{pu\times 1}$) is the q-th principal motion vector, whose eigenvalue is the q-th largest. Any motion can be approximated by a linear combination of principal motion vectors weighted by their corresponding scores:

$$\boldsymbol{x}_{c,k}^{(s)} \sim \boldsymbol{V}\boldsymbol{y}_{c,k}^{(s)}. \tag{5}$$

B. GENERALIZED PRINCIPAL MOTION ANALYSIS (GPMA)

We extended linear discriminant analysis to render it applicable to time-series data and propose generalized principal motion analysis (GPMA) [31]. GPMA includes basis functions that maximize the variation between factors, while reducing the variation within the factors. Therefore, this method can determine principal motions invariant with specific conditions such as the gait speed.

A matrix $\boldsymbol{B}$ ($\in \mathbb{R}^{s'c'\times pu}$) which exhibits the effects of the masked conditions within individuals is represented as follows:

$$\boldsymbol{B} = (\bar{\boldsymbol{x}}_1^{(1)} - \bar{\boldsymbol{x}}^{(1)}, \ldots, \bar{\boldsymbol{x}}_c^{(s)} - \bar{\boldsymbol{x}}^{(s)}, \ldots, \bar{\boldsymbol{x}}_{c'}^{(s')} - \bar{\boldsymbol{x}}^{(s')})^{\mathrm{T}}. \tag{6}$$

Here, $\bar{\boldsymbol{x}}_c^{(s)}$ represents the mean motion of participant s under condition c. Let the covariance matrices of $\boldsymbol{X}$ and $\boldsymbol{B}$ be

$\boldsymbol{S}$ ($= \boldsymbol{X}^{\mathrm{T}}\boldsymbol{X}$) and $\boldsymbol{D}$ ($= \boldsymbol{B}^{\mathrm{T}}\boldsymbol{B}$), respectively. We obtain a principal motion matrix and score matrix from the eigenvector expansion of matrix $\boldsymbol{D}^{-1}\boldsymbol{S}$. However, some of the principal motions obtained through this calculation cannot be interpreted because they are considerably affected by the masking effect of $\boldsymbol{D}$. Therefore, we extend GPMA to improve the interpretability of its principal motions. We obtain $\boldsymbol{D}_r$ by modifying $\boldsymbol{D}$ as

$$\boldsymbol{D}_r = \boldsymbol{D} + 10^{\alpha}\boldsymbol{I}. \tag{7}$$

Here, $\boldsymbol{I}$ ($\in \mathbb{R}^{pu\times pu}$) is a unit matrix, and coefficient α is an arbitrary real number. We can determine the intensity of the masking functions through the value of α. From the eigenvector expansion of matrix $\boldsymbol{D}_r^{-1}\boldsymbol{S}$, we obtain principal motion matrix $\boldsymbol{V}_g$ and score matrix $\boldsymbol{Y}_g$. When α is large, $\boldsymbol{V}_g$ is similar to $\boldsymbol{V}$, and GPMA and PMA are practically the same. On the other hand, when α is small, we can mask the effect of specific factors. As well as PMA, $\boldsymbol{x}_{c,k}^{(s)}$ is approximated by a linear combination of the principal motion vectors:

$$\boldsymbol{x}_{c,k}^{(s)} \sim \boldsymbol{V}_g \boldsymbol{y}_{g,c,k}^{(s)}. \tag{8}$$

III. GAIT VARIABILITY INDICES

A. PRINCIPAL MOTION ELLIPSOID (PM ELLIPSOID)

We use the size of the error (standard deviation) ellipsoid calculated individually from the distribution of the principal motion scores as the gait variability index (Fig. 1). Let this error ellipsoid be the principal motion ellipsoid (PM ellipsoid) [32]. The size of the PM ellipsoid represents the level of motion variability, whereas the direction represents how the motion varies. Suppose $q_m^{(s)}$ represents the length of the major axis m ($m = 1, \ldots, r$) of the PM ellipsoid for participant s, with r being the number of principal motions. We define the size of the PM ellipsoid for participant s as $e^{(s)}$ using the length of each axis, as follows:

$$e^{(s)} = \sum_{i=1}^{r} q_m^{(s)}. \tag{9}$$

Fig. 1 depicts the PM ellipsoid for participant s on the first–second principal motion plane as an example. Because the direction of the PM ellipsoid is nearly along the first principal motion, we can determine that the walking motion of participant s mainly varies for the first principal motion. Note that this ellipsoid is defined in an r-dimensional space.

B. MeanSD

The afore-mentioned gait variability indices evaluate different aspects of the walking motion. Hence, the correlation coefficients among them are small or null [7], [11], [40]. For example, the MeanSD evaluates the variability based on the standard deviation of the motion, whereas the maximum Lyapunov exponent evaluates the motion stability; hence, they are regarded independent. As there is high correlation between the PM ellipsoid and MeanSD [32], we use MeanSD as the reference index to investigate whether the PM ellipsoid computed using GPMA is valid as a gait variability index.

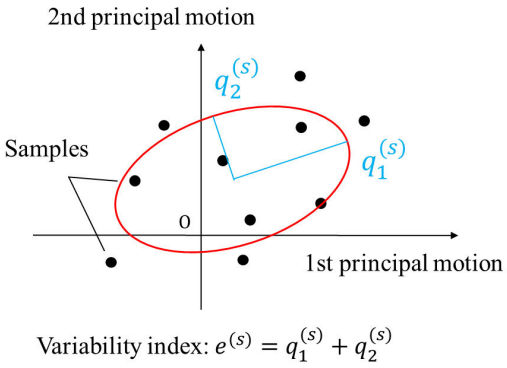

FIGURE 1. Definition of the size of the PM ellipsoid for participant *s*. The error ellipsoid (red) is calculated using the distributed samples (black dots).

MeanSD, which is the mean value of the standard deviation based on the gait cycle, has been used for the joint angle of the lower limbs [7], [37], [41], and for the velocity [2], [36], [37], [42] and acceleration [7], [40] obtained through an accelerometer attached to the waist.

For a participant, SD(l) represents the standard deviation at moment l on the gait cycle of a variable. Then, the MeanSD, which represents the gait variability for the entire gait cycle of the variable, is defined as

$$MeanSD = \langle SD(l)\,\rangle, l \in \{0, 1, \ldots, 100\%\ gait\ cycle\}, \tag{10}$$

where $\langle\,\rangle$ is the mean value of all the temporal points [7]. We calculated (10) for the six joint angles mentioned in Sec. 4.3, and defined their mean value as the MeanSD of the joint angle.

IV. WALKING MOTION EXPERIMENT

A. EXPERIMENT

In this study, we analyze the walking data measured by Ullauri *et al.* [43]; the relevant details can be found in the mentioned reference. A walking experiment was conducted on nine adult males (height: 172.5 $\pm$ 0.05 cm, weight: 63.6 $\pm$ 7.2 kg) without any neurological and musculoskeletal abnormalities.

B. METHOD

The gait motion was recorded at a frequency of 100 Hz using a motion capture system (MAC 3D system, Motion Analysis Corporation, U.S.) with ten cameras (nominal position resolution of submillimeter). Thirty-six reflective markers were attached on the entire body of the subject, as recommended by the motion module of the software for interactive musculoskeletal modeling (SIMM, Musculographics Inc., U.S.) used for calculating the joint angles. The participants walked on a treadmill with a 1.4×0.5 m^2 walking surface (OMEGA3, Johnson Health Tech Co., Taiwan).

Two walking trials with the different walking speed were recorded for each subject. To avoid exhaustion, the duration of each trial was set to 6 min. A speed of 1.11 m/s (4 km/h),

regarded as the natural walking speed of young adults, was selected as the regular walking speed, and a speed of 0.97 m/s (3.5 km/h) was selected as the slow speed.

C. MOTION DATA ANALYSIS

We visually inspected the motion samples used in [43] to confirm that there were no apparent erroneous gait motions. The first minute of all the gait motions in each trial was excluded from the analysis. All the data were smoothed using a 6-Hz Butterworth filter. From a single trial, we extracted 100 motions, defined as a gait cycle from the left-heel contact to the next left-heel contact in continuous walking. The gait cycle was normalized to 0–100% ($u = 101$) for aligning the data length of each trial (Fig. 2). The values of the joint angles were positive in the direction of flexing and negative in the direction of extending from the basic standing posture. We analyzed the hip flexion, knee flexion, and ankle dorsiflexion angles for the left and right legs. We defined the hip flexion angle as the angle between the vertical line passing through the hip joint and the straight line connecting the hip and knee joints.

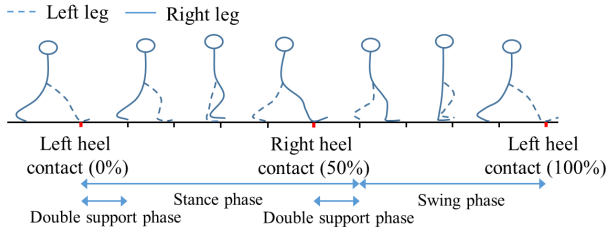

FIGURE 2. Gait cycle (defined from the left-heel contact (0%) to the next left-heel contact (100%)) normalized to 0–100%.

V. RESULTS

A. EFFECT OF GAIT SPEED ON THE PRINCIPAL MOTION SCORE

We confirmed the expression of the gait speed factor from the distribution of the principal motion score, within individuals. Table 1 presents the contribution ratio of the first–third principal motions in each motion analysis method. This ratio indicates the extent of variation in the samples for each principal motion. Even in earlier studies, gait motions have been expressed up to a few principal motions [19], [20], [24]. Fig. 3 displays the distribution of the principal motion score obtained using PMA (left), GPMA_2 (middle), and GPMA_{-7} (right). GPMA_α denotes GPMA with coefficient α. The reason for determining the value of α will be explained in Sec. V-C. The figures on top depict the first–second principal motion planes, whereas those on the bottom depict the second–third principal motion planes. The red and blue ellipses are the PM ellipsoids for gait speeds of 3.5 km/h and 4.0 km/h, respectively. The centroids of the sample distribution are represented as a marker for each participant.

The distances among the centroids in the score distribution between two gait-speed levels were maximum for PMA (left in Fig. 3), whereas they were almost matched for GPMA_{-7}. Those of GPMA_2 were moderately apart, between two gait-speed levels. These figures demonstrate that GPMA masks the gait-speed factor within individuals and α value adjusts the level of the masking function.

TABLE 1. Contribution ratio (%) of the first–third principal motions of PMA, GPMA_2, and GPMA_{-7}. PM: principal motion.

	PMA	GPMA_2	GPMA_{-7}
First PM	97.5	97.4	95.5
Second PM	0.91	0.88	1.32
Third PM	0.62	0.47	1.23

We investigated whether each principal motion was related to the gait speed through a t-test for the centroids of the score distribution between two gait speeds. The test statistics and p values are shown in Table 2. The first principal motion indicated no significant differences between the gait speeds in any analysis methods. For the second principal motion, the PMA scores when the participants walked at 4.0 km/h were greater than those at 3.5 km/h, which was not the case for GPMA. For the third principal motion, PMA exhibited marginal differences in the scores between the two gait-speed levels, i.e., 3.5 km/h $>$ 4.0 km/h, whereas the GPMA did not. Hence, the second and third principal motions of PMA depend on the gait speeds; however, those of GPMA do not, suggesting that GPMA extracts the principal motions invariant with speed.

TABLE 2. Test statistics and p values computed from the centroids of the score distribution between two gait speeds for each principal motion. If t is positive, the scores for 4.0 km/h are greater than those for 3.5 km/h.

	PMA	GPMA_2	GPMA_{-7}
First PM	$t(8) = 0.71$	$t(8) = 0.27$	$t(8) = 0.12$
	$p = 0.25$	$p = 0.40$	$p = 0.46$
Second PM	$t(8) = 2.10$	$t(8) = 0.03$	$t(8) = -0.03$
	$p = 0.04$	$p = 0.49$	$p = 0.49$
Third PM	$t(8) = -1.89$	$t(8) = 0.68$	$t(8) = 0.00$
	$p = 0.05$	$p = 0.47$	$p = 0.50$

To determine the speed dependence of MeanSD, we compared the MeanSD values between two speed levels. The mean and standard deviation of MeanSD among all the participants were 1.73 ± 0.23 deg and 1.80 ± 0.32 deg, for 3.5 and 4.0 km/h, respectively. There were no significant differences ($t(8) = 0.55$, $p = 0.30$) indicating that the MeanSD values were insensitive to the gait speed level in our data. This is not fully consistent with previous studies [37], [38], where MeanSD is sensitive to the gait speed. We discuss the reason for this in the first paragraph of Sec. VI.

B. CONCURRENT VALIDITY AS THE GAIT VARIABILITY INDEX

We compared the size of the PM ellipsoid obtained using each analysis method with the MeanSD, which is a representative gait variability index, and determined the concurrent validity of the PM ellipsoid as a gait variability index.

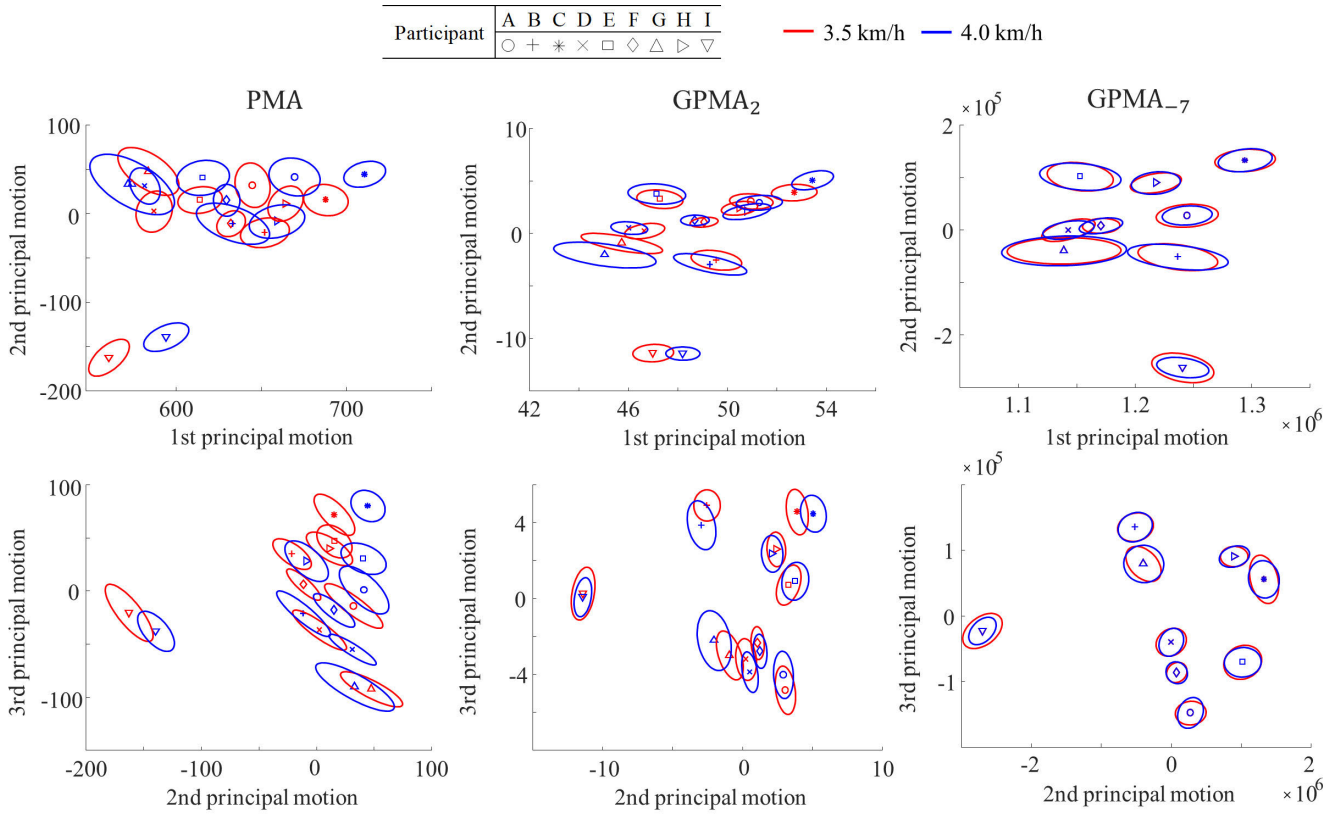

FIGURE 3. Scatter plots of the first–third principal motion scores of PMA (left), $GPMA_2$ (middle), and $GPMA_{-7}$ (right). Top: first–second principal motion planes; Bottom: second–third principal motion planes.

Table 3 represents the correlation coefficients between these indices. High correlation can be observed among all the cases, indicating that the MeanSD and size of the PM ellipsoid are similar indices for the degree of gait variability.

TABLE 3. Correlation coefficients between the MeanSD and size of the PM ellipsoid for PMA, $GPMA_2$, and $GPMA_{-7}$ at two gait speeds.

	PMA	$GPMA_2$	$GPMA_{-7}$
3.5 km/h	0.90	0.96	0.87
4.0 km/h	0.98	0.98	0.92

C. COMPARISON OF THE PMA- AND GPMA-ELLIPSOIDS

We verified the level to which the effect of the gait speed factor was masked for the gait variability level. We determined that the size of the PM ellipsoid, when participant s walked at a gait speed of c was $e_c^{(s)}$. Using the relative error, we defined an index representing the level to which the gait speed factor affects the size of the PM ellipsoid within individuals for each method as follows:

$$d^{(s)} = \left| \frac{e_{3.5}^{(s)}}{e_{4.0}^{(s)}} - 1 \right|. \tag{11}$$

When $d^{(s)}$ is close to zero, the effect of the gait speed is masked. Table 4 lists d computed for an individual, for each method. The mean values and standard errors of d of the nine participants for PMA, $GPMA_2$, and $GPMA_{-7}$ are 0.17 ± 0.02, 0.14 ± 0.03 and 0.10 ± 0.03, respectively. There are no significant differences in ds between PMA and $GPMA_2$ ($t(8) = -1.58, p > 0.05$), whereas d for $GPMA_{-7}$ tends to be lesser than that for PMA ($t(8) = -2.40, p < 0.05$, Bonferroni correction). Therefore, the PM ellipsoid based on $GPMA_{-7}$ is less sensitive to the gait speed factor for the gait variability level.

TABLE 4. Relative error of the principal motion ellipsoids (d) between two gait speeds. The values for $GPMA_2$ are comparable to those for PMA ($p = 0.154$), whereas those for $GPMA_{-7}$ are slightly smaller than those for PMA ($p = 0.043$).

	PMA	$GPMA_2$	$GPMA_{-7}$
Part.		d	
A	0.07	0.03	0.05
B	0.25	0.23	0.10
C	0.17	0.07	0.13
D	0.20	0.15	0.06
E	0.12	0.09	0.02
F	0.10	0.02	0.09
G	0.25	0.22	0.09
H	0.15	0.14	0.06
I	0.19	0.29	0.29
Mean	0.17	0.14	0.10
SE	0.02	0.03	0.03

Next, we verified the level to which the effect of the gait speed factor was masked in the direction of the PM ellipsoid by comparing the angles between the major axes of the

PM ellipsoids within individuals. We compared them on the first–second principal motion plane (ϕ_{1-2}) and second–third principal motion plane (ϕ_{2-3}). Table 5 presents ϕ_{1-2} and ϕ_{2-3} computed through each method. The mean values and standard errors of ϕ_{1-2} of the nine participants for PMA, $GPMA_2$, and $GPMA_{-7}$ are 20.0 ± 6.77, 27.1 ± 7.37,, and 12.2 ± 2.24, respectively, and those of ϕ_{2-3} are 6.58 ± 1.94, 12.2 ± 6.87, and 26.3 ± 6.53, respectively. There are no significant differences among these values except for ϕ_{2-3} between PMA and $GPMA_{-7}$ ($t(8) = -3.10, p < 0.05$). The masking ability of GPMA did not affect the PM ellipsoid direction.

TABLE 5. Differences in the degrees of the principal motion ellipsoids between two gait speeds, calculated on the first–second principal motion plane (ϕ_{1-2}) and second–third principal motion plane (ϕ_{2-3}).

	PMA		$GPMA_2$		$GPMA_{-7}$	
Part.	ϕ_{1-2}	ϕ_{2-3}	ϕ_{1-2}	ϕ_{2-3}	ϕ_{1-2}	ϕ_{2-3}
A	7.56	8.05	32.1	6.89	2.46	63.0
B	66.8	3.70	6.08	64.9	8.89	12.9
C	38.6	4.69	36.1	19.6	20.5	4.89
D	13.8	3.84	60.1	4.92	13.1	25.2
E	7.92	19.8	18.2	3.99	20.3	29.9
F	10.9	4.59	24.9	1.87	10.3	52.0
G	4.01	2.54	4.37	7.17	2.82	22.3
H	19.1	11.1	3.02	0.74	15.0	18.3
I	11.0	0.82	58.6	0.08	16.7	8.08
Mean	20.0	6.58	27.1	12.2	12.2	26.3
SE	6.77	1.94	7.37	6.87	2.24	6.53

Fig. 4 depicts the mean values of d for the nine participants, when α is varied by 0.1. It can be observed that the mean values of d vary considerably for $0 < \alpha < 4$. The mean value of d for $GPMA_7$ is 0.165, indicating that $GPMA_7$ has a low masking ability similar to PMA with $d = 0.167$. The mean value of d for $GPMA_{-7}$ is 0.10. The mean value of d is 0.13, when α is approximately two, indicating that the masking ability of $GPMA_2$ is between those of PMA and $GPMA_{-7}$.

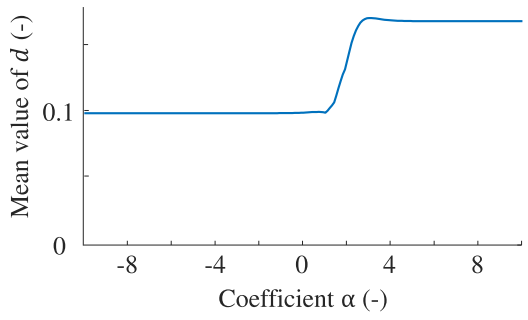

FIGURE 4. Relationship between the mean value of d (relative error of the ellipsoidal sizes between 3.5 km/h and 4.0 km/h) and masking coefficient α.

VI. DISCUSSION

In Sec. V, we demonstrated that the PM ellipsoids based on GPMA and the MeanSD, a popular gait variability index, exhibited correlation coefficients greater than 0.87. Furthermore, the principal motion scores of GPMA and the size of the GPMA-based ellipsoid do not depend on the gait speed, in contrast to those based on PMA. These results indicate that the PM ellipsoids computed using GPMA function as a gait variability index invariant with the gait speed, whereas the other popular gait variability indices are influenced by the gait speed, as previously mentioned in Sec. I. Nonetheless, the MeanSD values did not differ among the two speed levels for our gait samples. The possible reason is as follows: The gait variability index can be a quadratic U-shaped function of the gait speed with minimum values at the potentially preferred speed [38], [44]–[46]. The gait speeds in this study were within the range of the participants' preferred speed, and the speed-dependency of the MeanSD may have been concealed.

A. INTERPRETATION OF THE PRINCIPAL MOTIONS

We may understand the variation in the walking motion within individuals by interpreting each principal motion. Fig. 5 shows the time-series change of the load of the first–third principal motions obtained using PMA, $GPMA_2$, and $GPMA_{-7}$. As the load represents the flexion of the joint angles, if the load is zero, the flexion angle is zero, and if the load is positive or negative, the joint angle flexes or extends. Further, Fig. 6 shows the average joint motions during a gait cycle, which helps in interpreting the principal motions.

1) PRINCIPAL MOTION ANALYSIS

Fig. 5 (a), which is the first principal motion of PMA, indicates that the knee joints flex (positive), hip joints flex (positive), and ankle joints plantarflex (negative) during the first half of the swing phase of both legs. These represent typical walking motion because they resemble the average joint motion in Fig. 6. Therefore, we can interpret the first principal motion as average walking motion or the degree of entire gait motion. The variance of the gait samples along the first principal motion is greater than those along the other principal motions suggesting that the variance of walking motion is mainly the degree of the entire joint motion.

Fig. 5 (b), which is the second principal motion, shows that the hip and knee joints flex (positive), and the ankle joints plantarflex (negative) during the first half of the swing phase, whereas the knee joints extend (negative) during the second half of the swing phase for both legs. This motion can be considered to represent the advance of the gait phase because it appears as the differential motion of the average walking motion in Fig. 6. Fig. 7 depicts the knee flexion angles of gait samples with the maximum and minimum scores for the second principal motion, for a participant. Gait samples with the maximum scores for the second principal motion shift to the swing phase earlier than the minimum ones. Therefore, the second principal motion also represents walking motion with long swing phases. As shown in Table 2 in Sec. 5.1, the second principal motion is related to the gait speed, and gait samples at 4.0 km/h have larger scores for this principal motion than those at 3.5 km/h. People, who walk faster, have longer swing phases [19], [43].

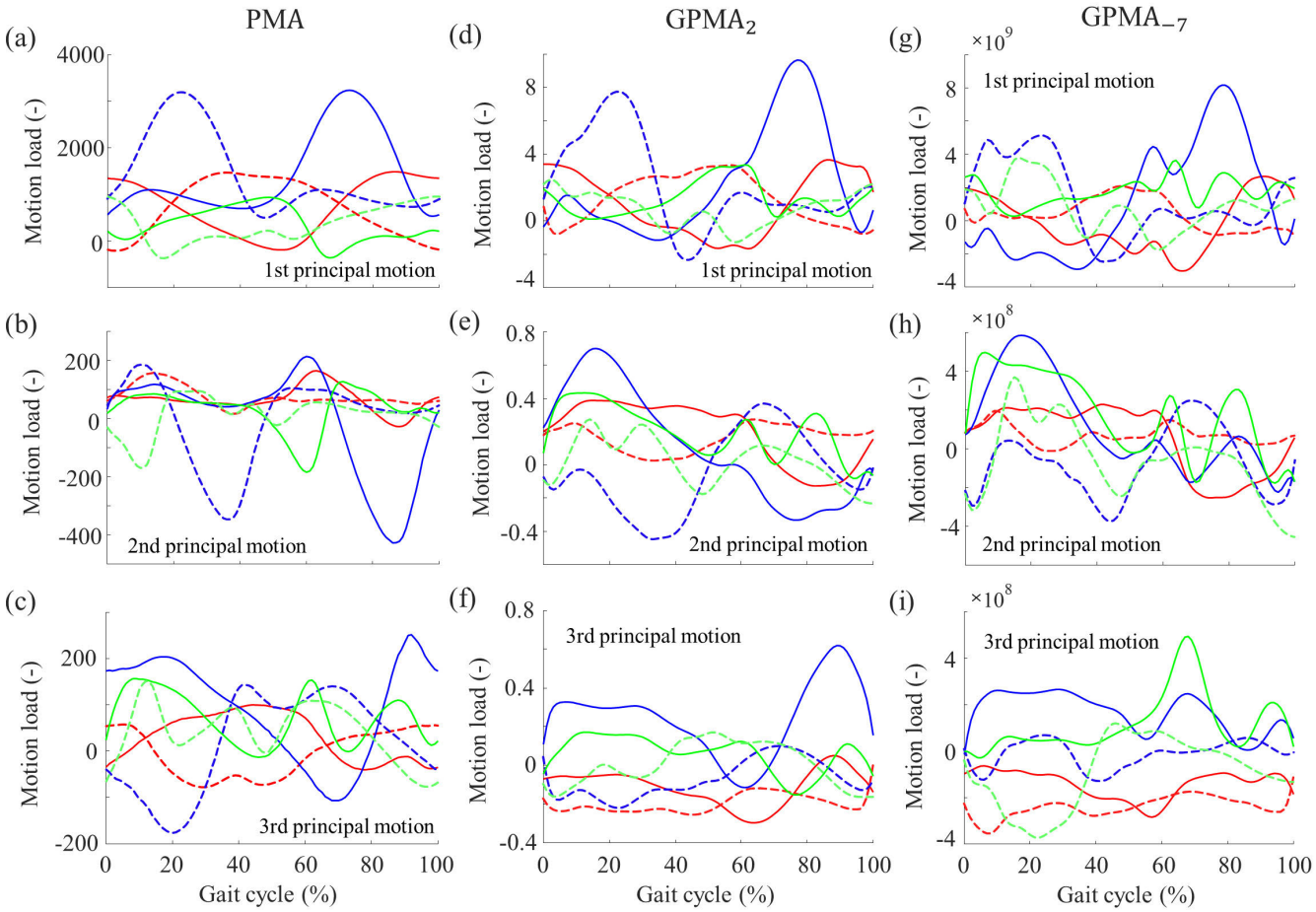

FIGURE 5. Load of each principal motion of PMA (left), $GPMA_2$ (middle), and $GPMA_{-7}$ (right) computed using the joint angles. Top: first principal motion; Middle: second principal motion; Bottom: third principal motion.

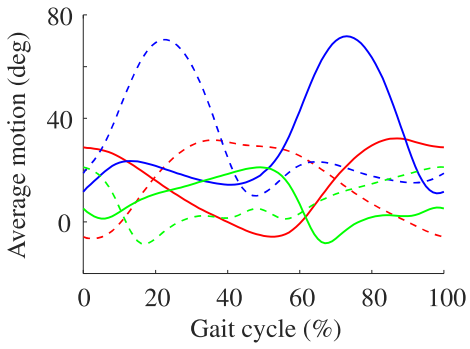

FIGURE 6. Average joint motion during a gait cycle.

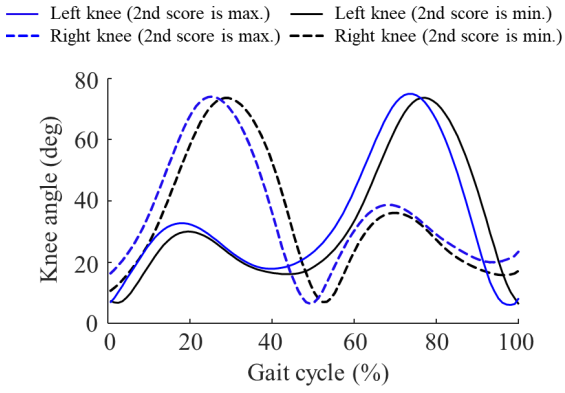

FIGURE 7. Gait samples with maximum (blue line) and minimum (black line) scores for the second principal motion of PMA. Solid line: left-knee angle; Dotted line: right-knee angle.

Fig. 5 (c), which is the third principal motion, shows that the knee joint of the stance leg flexes (positive) and the swing leg extends (negative) at heel contact, after which the hip joint of the stance leg flexes (positive) and the swing leg extends (negative) for both legs. As in Table 2, this principal motion is related to the gait speed. Similar to [43], our data indicates that the gait-speed factor affects the length of the swing phase and step length. In PMA, as mentioned in the previous paragraph, the second principal motion represents the length of the swing phase. Hence, it is considered that the third principal motion can be related to the step length. People, who walk fast, have large step lengths as per our

data [43]. Participants with large scores for this principal motion tend to walk slowly, as depicted in Table 2, and the scores of this principal motion are moderately correlated with the step length ($r = -0.317, t = 14.96, p < 0.001$). Samples with the greater scores tend to involve slower motions with smaller step lengths.

2) GENERALIZED PRINCIPAL MOTION ANALYSIS ($\alpha = 2$)

Here, we interpret the principal motions obtained using GPMA_2. Although it is occasionally difficult to interpret the principal motions of GPMA because they contain high-frequency components, we may be able to infer their meanings from similar principal motions of PMA. We smoothened the principal motions using a Gaussian filter with a length of ten for visual clarity in Fig. 5.

Fig. 5 (d), which is the first principal motion, resembles the first principal motion of PMA. Therefore, it is considered to represent average walking motion.

Fig. 5 (e), which is the second principal motion, shows that the left knee joint flexes (positive) during the first half of the stance phase, becomes zero at approximately 50% of the gait cycle, and extends in the swing phase. The right knee joint is around zero during the first half of the swing phase, extends (negative) during 20%–50% of the gait cycle, and flexes (positive) during the stance phase. The hip joints flex (positive) in the stance phase and extend (negative or zero) in the swing phase of both legs. This shows the left-right asymmetry of walking, suggesting that the double stance phase of right-heel contact—left-toe off is longer than that of left-heel contact—right-toe off. Fig. 8 shows the knee flexion angles of two gait samples with the maximum and minimum scores, respectively, of the second principal motion for a certain participant. In this example, the gait sample with the maximum score for the second principal motion (blue curves) exhibits peak left and right knee flexion angles at 18% and 72%, respectively. The difference in phase between these two peaks is 54%. In contrast, the gait sample with the least score (black curves) exhibits peak left and right knee angles at 21% and 67%, respectively, resulting in a phase difference of 46%. As such, the second principal motion pertains to the left-right asymmetry of motion.

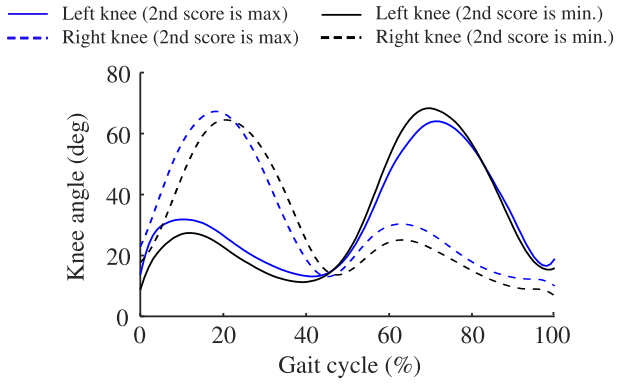

FIGURE 8. Gait samples with maximum (blue line) and minimum (black line) scores for the second principal motion of GPMA_2. Solid line: left-knee angle; Dotted line: right-knee angle.

Fig. 5 (f), which is the third principal motion, is difficult to interpret because of its complexity, but it resembles the third principal motion of PMA, relatively. However, as in Table 2, the third principal motion of GPMA_2 is invariant with the gait speed, whereas that of PMA is sensitive to the gait speed.

3) GENERALIZED PRINCIPAL MOTION ANALYSIS ($\alpha = -7$)

The principal motions obtained through GPMA_{-7} are considerably different from those of PMA and GPMA_2, and are difficult to interpret.

The first principal motion (Fig. 5 (g)) resembles that of PMA and GPMA_2, relatively. Therefore, it may represent average walking motion.

The second principal motion of GPMA_{-7} (Fig. 5 (h)) resembles that of GPMA_2, partially. From this point of view, it may represent the left-right asymmetry of the double stance phases.

The third principal motion of GPMA_{-7} (Fig. 5 (i)) does not resemble any of the principal motions of PMA and GPMA_2. Further, the joint profiles differ among the first and second halves of the gait cycle, indicating laterally asymmetric motion. However, this principal motion could not be directly interpreted.

B. LIMITATIONS OF PM ELLIPSOIDS AND THIS PRESENT STUDY

As indicated in Sec. V-B, the MeanSD and size of the PM ellipsoid are similar indices for the degree of gait variability. As mentioned in Sec. III-B, some of the representative gait variability indices do not exhibit high correlation coefficients with each other because they are based on inherently different aspects of walking motions [7], [11], [40]. Hence, it is considered that the correlation coefficient between the size of the PM ellipsoid and the other gait variability indices, including the maximum Lyapunov component, is small. This is a common problem in gait variability indices.

PM ellipsoids consider the motion repetition error as variability. When PMA or GPMA is applied to motions, except walking, the motion start and finish points need to be clearly defined, in continuously recorded motions. Thus, aperiodic motion or motion with no apparent cycle is unsuitable for analysis. Further, although this study targeted the gait variability of healthy participants, it is important to investigate whether PM ellipsoids are available for gait with abnormality because gait fluctuation is the key for analyzing such gait patterns [12]–[14]. This remains to be studied in future. Similarly, although we expect that our method is applicable to extremely slow or fast walking motions, this study considers only the typical gait speed range; this aspect also needs to be demonstrated in future.

As shown in Fig. 3, GPMA can mask the effect of the gait speed factor within individuals because the distances among the centroids of the scores between two gait speed

levels are smaller than those of PMA. Furthermore, as Table 4 shows, GPMA can mask the effect of gait speed on the degree of individual gait variability. On the other hand, there were no significant differences between PMA and GPMA for the direction of the PM ellipsoid, as indicated by Table 5. In this study, as in (6), we defined the effect of the gait speed as the difference between the mean motions at 3.5 and 4.0 km/h. Hence, the difference between the mean motions for the two gait speed levels can be masked by GPMA, but it does not mask the effect of the gait speed level on the directions of the PM ellipsoids.

As previously mentioned, GPMA-based PM ellipsoids employ the difference between the mean motions of the two gait speed levels to mask the effect of the gait speed factor. If the gait speeds are discrete, as in 3.5 km/h and 4.0 km/h, we can analyze the variability between them; however, this cannot be done, if the gait speeds vary continuously.

VII. CONCLUSION

In this study, we developed a new index for gait variability using GPMA, which is an extended PMA method, that can mask the effect of a certain factor for computing the principal motions. This index is based on the variability ellipsoids of motion samples in the principal motion space. Hence, it provides the magnitude and properties of motion variability, unlike previous gait variability indices. Furthermore, we modified the previously proposed GPMA by introducing a function to adjust the masking ability of GPMA. Using PMA and GPMA, we computed the PM ellipsoids of the walking motions recorded at two gait-speed levels. The GPMA ellipsoids were less sensitive to the gait speed than the PMA ellipsoids, as indicated by the distance among the centroids of the score distribution between the gait speeds and the size of the PM ellipsoid within individuals. Ellipsoids computed using PMA and GPMA exhibited high correlation coefficients with the MeanSD, which is a representative gait variability index. Furthermore, we demonstrated that the interpretation of the principal motions can be easier by adjusting the masking capability of GPMA. A PM ellipsoid based on GPMA is a useful variability index because it indicates the degree of gait variability and the variation in individual gait motion, with the ability to mask the effect of experimental factors such as the gait speed.

REFERENCES

[1] S. A. England and K. P. Granata, "The influence of gait speed on local dynamic stability of walking," *Gait Posture*, vol. 25, no. 2, pp. 172–178, Feb. 2007.
[2] S. M. Bruijn, J. H. van Dieën, O. G. Meijer, and P. J. Beek, "Is slow walking more stable?" *J. Biomech.*, vol. 42, no. 10, pp. 1506–1512, Jul. 2009.
[3] T. M. Owings and M. D. Grabiner, "Variability of step kinematics in young and older adults," *Gait Posture*, vol. 20, no. 1, pp. 26–29, Aug. 2004.
[4] L. Hak, H. Houdijk, P. J. Beek, and J. H. van Dieën, "Steps to take to enhance gait stability: The effect of stride frequency, stride length, and walking speed on local dynamic stability and margins of stability," *PLoS ONE*, vol. 8, no. 12, Dec. 2013, Art. no. e82842.
[5] Y. Akiyama, H. Toda, T. Ogura, S. Okamoto, and Y. Yamada, "Classification and analysis of the natural corner curving motion of humans based on gait motion," *Gait Posture*, vol. 60, pp. 15–21, Feb. 2018.
[6] Y. Akiyama, S. Okamoto, H. Toda, T. Ogura, and Y. Yamada, "Gait motion for naturally curving variously shaped corners," *Adv. Robot.*, vol. 32, no. 2, pp. 77–88, Jan. 2018.
[7] J. B. Dingwell, J. P. Cusumano, P. R. Cavanagh, and D. Sternad, "Local dynamic stability versus kinematic variability of continuous overground and treadmill walking," *J. Biomechanical Eng.*, vol. 123, no. 1, pp. 27–32, Feb. 2001.
[8] J. B. Dingwell and J. P. Cusumano, "Nonlinear time series analysis of normal and pathological human walking," *Interdiscipl. J. Nonlinear Sci.*, vol. 10, no. 4, pp. 848–863, Dec. 2000.
[9] M. Costa, C.-K. Peng, A. L. Goldberger, and J. M. Hausdorff, "Multiscale entropy analysis of human gait dynamics," *Phys. A, Stat. Mech. Appl.*, vol. 330, nos. 1–2, pp. 53–60, Dec. 2003.
[10] F. Sylos Labini, A. Meli, Y. P. Ivanenko, and D. Tufarelli, "Recurrence quantification analysis of gait in normal and hypovestibular subjects," *Gait Posture*, vol. 35, no. 1, pp. 48–55, Jan. 2012.
[11] F. Riva, M. C. Bisi, and R. Stagni, "Gait variability and stability measures: Minimum number of strides and within-session reliability," *Comput. Biol. Med.*, vol. 50, pp. 9–13, Jul. 2014.
[12] S. Qiu, L. Liu, Z. Wang, S. Li, H. Zhao, J. Wang, J. Li, and K. Tang, "Body sensor network-based gait quality assessment for clinical decision-support via multi-sensor fusion," *IEEE Access*, vol. 7, pp. 59884–59894, 2019.
[13] Y. Yan, O. M. Omisore, Y. Xue, H. Li, Q. Liu, Z. Nie, J. Fan, and L. Wang, "Classification of neurodegenerative diseases via topological motion analysis—A comparison study for multiple gait fluctuations," *IEEE Access*, vol. 8, pp. 96363–96377, 2020.
[14] Y. Moon, J. Sung, R. An, M. E. Hernandez, and J. J. Sosnoff, "Gait variability in people with neurological disorders: A systematic review and meta-analysis," *Hum. Movement Sci.*, vol. 47, pp. 197–208, Jun. 2016.
[15] F. C. Park and K. Jo, "Movement primitives and principal component analysis," in *On Advances in Robot Kinematics*. Dordrecht, The Netherlands: Springer, 2004, pp. 97–106.
[16] B. Lim, S. Ra, and F. C. Park, "Movement primitives, principal component analysis, and the efficient generation of natural motions," in *Proc. IEEE Int. Conf. Robot. Autom.*, Apr. 2005, pp. 4630–4635.
[17] Z.-M. Li and J. Tang, "Coordination of thumb joints during opposition," *J. Biomechan.*, vol. 40, no. 3, pp. 502–510, Jan. 2007.
[18] N. St-Onge and A. G. Feldman, "Interjoint coordination in lower limbs during different movements in humans," *Exp. Brain Res.*, vol. 148, no. 2, pp. 139–149, Jan. 2003.
[19] N. A. Borghese, L. Bianchi, and F. Lacquaniti, "Kinematic determinants of human locomotion," *J. Physiol.*, vol. 494, no. 3, pp. 863–879, 1996.
[20] C. D. Mah, M. Hulliger, R. G. Lee, and I. S. O'Callaghan, "Quantitative analysis of human movement synergies: Constructive pattern analysis for gait," *J. Motor Behav.*, vol. 26, no. 2, pp. 83–102, Jun. 1994.
[21] T. Funato, S. Aoi, H. Oshima, and K. Tsuchiya, "Variant and invariant patterns embedded in human locomotion through whole body kinematic coordination," *Exp. Brain Res.*, vol. 205, no. 4, pp. 497–511, Sep. 2010.
[22] S. Vernazza-Martin, N. Martin, and J. Massion, "Kinematic synergies and equilibrium control during trunk movement under loaded and unloaded conditions," *Exp. Brain Res.*, vol. 128, no. 4, pp. 517–526, Oct. 1999.
[23] T. Funato, S. Aoi, N. Tomita, and K. Tsuchiya, "Human gait control suggested by the evaluation of the fluctuation of synergy," in *Proc. IEEE/SICE Int. Symp. Syst. Integr. (SII)*, Dec. 2011, pp. 267–272.
[24] H. Oshima, S. Aoi, T. Funato, N. Tsujiuchi, and K. Tsuchiya, "Variant and invariant spatiotemporal structures in kinematic coordination to regulate speed during walking and running," *Frontiers Comput. Neurosci.*, vol. 13, p. 63, Sep. 2019.
[25] K. Fujii, N. Takeishi, B. Kibushi, M. Kouzaki, and Y. Kawahara, "Data-driven spectral analysis for coordinative structures in periodic human locomotion," *Sci. Rep.*, vol. 9, no. 1, pp. 1–14, Dec. 2019.
[26] K. Mishima, S. Kanata, H. Nakanishi, T. Sawaragi, and Y. Horiguchi, "Extraction of similarities and differences in human behavior using singular value decomposition," *IFAC Proc. Vols.*, vol. 43, no. 13, pp. 436–441, 2010.
[27] H. Kang and F. C. Park, "Humanoid motion optimization via nonlinear dimension reduction," in *Proc. IEEE Int. Conf. Robot. Autom.*, May 2012, pp. 1444–1449.
[28] S. Morishima, K. Ayusawa, E. Yoshida, and G. Venture, "Whole-body motion retargeting using constrained smoothing and functional principle component analysis," in *Proc. IEEE-RAS 16th Int. Conf. Humanoid Robots (Humanoids)*, Nov. 2016, pp. 294–299.

[29] T. Akiduki, K. Kawamura, Z. Zhang, and H. Takahashi, "Extraction and classification of human gait features from acceleration data," *Int. J. Innov. Comput., Inf. Control*, vol. 14, no. 4, pp. 1361–1370, 2018.
[30] T. Akiduki, A. Uchida, Z. Zhang, T. Imamura, and H. Takahashi, "Extraction of human gait feature from acceleration data," *ICIC Exp. Lett., B, Appl.*, vol. 7, no. 3, pp. 649–656, 2016.
[31] T. Iwasaki, S. Okamoto, Y. Akiyama, and Y. Yamada, "Generalized principal motion analysis: Classification of Sit-to-Stand motions," in *Proc. IEEE 8th Global Conf. Consum. Electron. (GCCE)*, Oct. 2019, pp. 679–681.
[32] T. Iwasaki, S. Okamoto, Y. Akiyama, and Y. Yamada, "Principal motion ellipsoids: Gait variability index based on principal motion analysis," in *Proc. IEEE/SICE Int. Symp. Syst. Integr. (SII)*, Jan. 2020, pp. 489–494.
[33] J. M. Hausdorff, M. E. Cudkowicz, R. Firtion, J. Y. Wei, and A. L. Goldberger, "Gait variability and basal ganglia disorders: Stride-to-stride variations of gait cycle timing in parkinson's disease and Huntington's disease," *Movement Disorders*, vol. 13, no. 3, pp. 428–437, May 1998.
[34] K. Jordan, J. H. Challis, and K. M. Newell, "Walking speed influences on gait cycle variability," *Gait Posture*, vol. 26, no. 1, pp. 128–134, Jun. 2007.
[35] M. D. Latt, H. B. Menz, V. S. Fung, and S. R. Lord, "Walking speed, cadence and step length are selected to optimize the stability of head and pelvis accelerations," *Exp. Brain Res.*, vol. 184, no. 2, pp. 201–209, Nov. 2007.
[36] J. B. Dingwell and L. C. Marin, "Kinematic variability and local dynamic stability of upper body motions when walking at different speeds," *J. Biomech.*, vol. 39, no. 3, pp. 444–452, Jan. 2006.
[37] H. G. Kang and J. B. Dingwell, "Separating the effects of age and walking speed on gait variability," *Gait Posture*, vol. 27, no. 4, pp. 572–577, May 2008.
[38] M. Yamasaki, T. Sasaki, and M. Torii, "Sex difference in the pattern of lower limb movement during treadmill walking," *Eur. J. Appl. Physiol. Occupational Physiol.*, vol. 62, no. 2, pp. 99–103, 1991.
[39] J. L. Helbostad and R. Moe-Nilssen, "The effect of gait speed on lateral balance control during walking in healthy elderly," *Gait Posture*, vol. 18, no. 2, pp. 27–36, Oct. 2003.
[40] P. Terrier and O. Dériaz, "Kinematic variability, fractal dynamics and local dynamic stability of treadmill walking," *J. NeuroEngineering Rehabil.*, vol. 8, no. 1, p. 12, Dec. 2011.
[41] D. H. Gates, B. J. Darter, J. B. Dingwell, and J. M. Wilken, "Comparison of walking overground and in a computer assisted rehabilitation environment (CAREN) in individuals with and without transtibial amputation," *J. NeuroEngineering Rehabil.*, vol. 9, no. 1, p. 81, 2012.
[42] M. Punt, S. M. Bruijn, H. Wittink, and J. H. van Dieën, "Effect of arm swing strategy on local dynamic stability of human gait," *Gait Posture*, vol. 41, no. 2, pp. 504–509, Feb. 2015.
[43] J. B. Ullauri, Y. Akiyama, S. Okamoto, and Y. Yamada, "Technique to reduce the minimum toe clearance of young adults during walking to simulate the risk of tripping of the elderly," *PLoS ONE*, vol. 14, no. 6, Jun. 2019, Art. no. e0217336.
[44] F. Danion, E. Varraine, M. Bonnard, and J. Pailhous, "Stride variability in human gait: The effect of stride frequency and stride length," *Gait Posture*, vol. 18, no. 1, pp. 69–77, Aug. 2003.
[45] J. M. Hausdorff, "Stride variability: Beyond length and frequency," *Gait Posture*, vol. 20, no. 3, p. 304, Dec. 2004.
[46] J. M. Hausdorff, "Gait variability: Methods, modeling and meaning," *J. NeuroEng. Rehabil.*, vol. 2, p. 19, Dec. 2005.

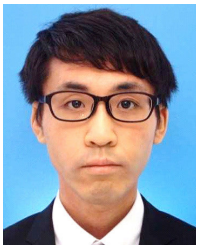

TOMOYUKI IWASAKI received the B.S. degree from Nagoya University, in 2019, where he is currently pursuing the degree with the Department of Mechanical Systems Engineering.

SHOGO OKAMOTO (Member, IEEE) received the Ph.D. degree in information sciences from Tohoku University, in 2010. Since 2010, he has been with Nagoya University. He is currently an Associate Professor with the Department of Mechanical Systems Engineering, Nagoya University. His research interests include haptics, assistive robotics, and affective engineering.

YASUHIRO AKIYAMA (Member, IEEE) received the B.E. degree in engineering from the Tokyo Institute of Technology, Tokyo, Japan, in 2006, and the M.S. and Ph.D. degrees in engineering from the University of Tokyo, Tokyo, in 2008 and 2011, respectively. Since 2016, he has been an Assistant Professor with Nagoya University, Japan. His main research interests include mechanical safety, human–robot interaction, and biomechanics.

YOJI YAMADA (Member, IEEE) received the Ph.D. degree from the Tokyo Institute of Technology. Since 1983, he has been with the Toyota Technological Institute, Nagoya, Japan. In 2004, he joined the National Institute of Advanced Industrial and Science Technology (AIST), as a Leader of the Safety Intelligence Research Group. In 2009, he moved to the Department of Mechanical Science and Engineering, Graduate School of Engineering, Nagoya University, as a Professor.